DALTON
FULL PAPER

Electronic effects in the nickel-catalysed hydrocyanation of styrene applying chelating phosphorus ligands with large bite angles‡

Wolfgang Goertz,[a] Wilhelm Keim,[a] Dieter Vogt,*,†,[a] Ulli Englert,[b] Maarten D. K. Boele,[c] Lars A. van der Veen,[c] Paul C. J. Kamer[c] and Piet W. N. M. van Leeuwen[c]

[a] *Institut für Technische Chemie und Petrolchemie, RWTH Aachen, Templergraben 55, 52056 Aachen, Germany*
[b] *Institut für Anorganische Chemie, RWTH Aachen, Templergraben 55, 52056 Aachen, Germany*
[c] *J. H. van't Hoff Research Institute, Department of Inorganic Chemistry, University of Amsterdam, Nieuwe Achtergracht 166, 1018 WV Amsterdam, The Netherlands*

Chelating phosphorus ligands with a rigid backbone and a large natural bite angle were applied in the nickel-catalysed hydrocyanation of styrene. The *para* substituents in the diphenylphosphanyl moiety of the 4,6-bis-(diphenylphosphanyl)-2,8-dimethylphenoxathiine (Thixantphos) ligands were varied and their electronic effects on the activity and selectivity of the catalytic experiments were investigated. The activity of the nickel complexes decreased when electron-donating substituents lead to a more basic phosphorus while electron-withdrawing substituents led to a higher activity. The results of variable temperature ^{31}P-{^{1}H} NMR experiments on the *in situ* catalysts are discussed in relationship to the catalytic performance. 4,6-Bis(diphenylphosphanyl)-2,8-dimethylphenoxathiine (Thixantphos) L^{1d} and the complexes [$NiCl_2L^{1d}$] **1** and [$Ni(CN)_2L^{1a}$] **2** (*p*-Me_2N on phenyl) have been characterised by single-crystal X-ray diffraction. Complex **2** represents the first crystal structure of a monomeric dicyanonickel(II) complex with a P–P chelating ligand. The geometries of ligand L^{1d} and complex **1** were predicted by molecular mechanics calculations.

The hydrocyanation of butadiene in the presence of nickel complexes, known as the DuPont ADN Process, is one of the most prominent examples of homogeneous catalysis on an industrial scale.[1] Many investigations have been undertaken to understand its mechanism and to improve the activity and selectivity.[2] For some decades the process has been carried out with monodentate phosphites which are bound only very weakly to the zerovalent metal centre.[3] For this reason, one major drawback in this process arises from the formation of inactive nickel cyanides when the monodentate ligands dissociate and the catalyst metal is exposed to an excess of HCN. Only recently bidentate ligands have drawn some attention.[4] They are able to stabilise the active species to a much higher extent due to the chelate effect. It was reported by Pringle and co-workers[5] that diphosphites form complexes with nickel and palladium, that are active in hydrocyanation catalysis and highly resistant towards oxidation as well. Striking results have been obtained in the asymmetric hydrocyanation of vinylarenes by using chiral diphosphinites derived from sugar backbones.[6] Enantiomeric excesses up to 95% combined with high activities were achieved.[7] It was suggested that the enantioselectivity of the reaction is determined in the reductive elimination step of the catalytic cycle which is strongly influenced by the electronic properties of the ligand.

In preliminary communications, we have reported on the successful application of diphosphines in the hydrocyanation of styrene[8] and long-chain, non-activated olefins.[9] These newly developed Xantphos ligands[10] have large natural bite angles and rigid backbones. The compounds are based on heterocyclic xanthene-like aromatics. They were designed to stabilise geometries with P–Ni–P angles larger than 100°, shown to have a strong influence on catalyst selectivity in manifold reactions.[10,11] By modifying the ligand backbone the bite angle can be precisely adjusted to various geometries. For the catalytic hydrocyanation we proposed that ligands with fixed large bite angles would (a) disfavour inactive square planar nickel(II) dicyano species, and (b) stabilise active tetrahedral nickel(0) complexes.[8]

Next to the geometry of the ligands, their electronic properties play a crucial role for the complex stability and have a great influence on elementary steps of the catalytic cycle.[12] Ligands with electron-withdrawing substituents at the phosphorus atoms bear a low basicity and can easily compensate the high electron density of the d^{10} configurated zerovalent nickel by back donation into non-occupied orbitals. A nickel which is electron-poor due to ligand properties will readily co-ordinate an olefinic substrate. Moreover, kinetic studies by RajanBabu[6] and co-workers indicate that the rate of reductive elimination is increased by electron-withdrawing substituents at the ligand. For these reasons, phosphites with three electron-withdrawing oxygen substituents are much more favourable for hydrocyanation reactions than phosphines. However, we could demonstrate that Xantphos type diphosphines are quite comparably active to monophosphites.[8,9]

In this paper we describe the application of electronically tuned Thixantphos type ligands L^{1a}–L^{1g} and L^{2b} (Scheme 1) in the hydrocyanation of styrene. Substituents were introduced in the *para* positions of the phenyl rings only in order to keep steric effects as small as possible. In this way it should be possible to study the electronic effects independently from the bite angle. Natural bite angles for nickel complexes and other ligand geometries were calculated by molecular modeling, using an augmented TRIPOS force field with SYBYL software.[13] The natural bite angle is defined as the preferred chelation angle determined only by ligand-backbone constraints and not by metal valence angles.[14] We have studied the crystal structures of one free Thixantphos L^{1d} (R = H) and two nickel complexes [$NiCl_2L^{1d}$] **1** and [$Ni(CN)_2L^{1a}$] **2** to support the suggested relationship between the geometry and the reactivity of

† E-Mail: dieter.vogt@post.rwth-aachen.de
‡ *Supplementary data available*: computational and other details. For direct electronic access see http://www.rsc.org/suppdata/dt/1998/2981/, otherwise available from BLDSC (No. SUP 57410, 5 pp.) or the RSC Library. See Instructions for Authors, 1998, Issue 1 (http://www.rsc.org/dalton).

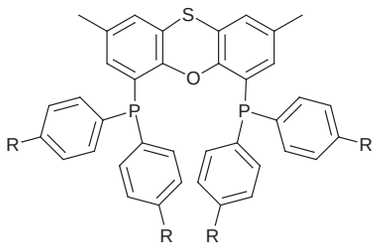

P—P	R	β_n /°
L^{1a}	Me_2N	118.6
L^{1b}	MeO	113.8
L^{1c}	Me	112.9
L^{1d}	H	112.8
L^{1e}	F	112.8
L^{1f}	Cl	113.4
L^{1g}	CF_3	114.5

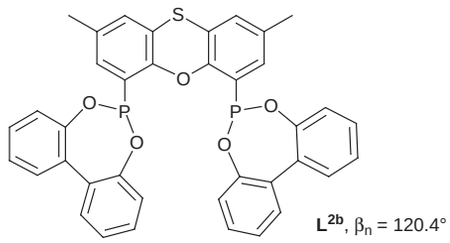

Scheme 1 Thixantphos ligands and their calculated natural bite angles

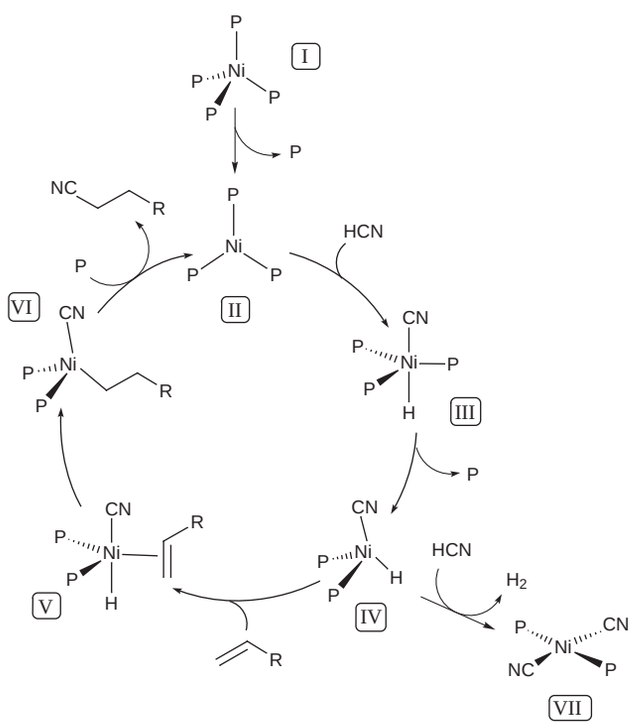

Species	Geometry	Angle P - Ni - P
I, IV, VI	tetrahedral	109°
II	trigonal	120°
III, V	trigonal-bipyramidal	120°
VII	square-planar	90/180°

Scheme 2 Proposed catalytic cycle for hydrocyanation

catalytically active intermediates. We have also carried out $^{31}P\{^1H\}$ NMR investigations with the *in situ* catalysts which provide useful information on the performance and deactivation pathways for the various nickel complexes.

Results and Discussion

Mechanistic aspects

The catalytic cycle for the hydrocyanation of olefins applying monodentate phosphorus ligands P as shown in Scheme 2 has been proposed by Tolman *et al.*[15] Intermediates and catalytically active species have been isolated or observed and characterised by various spectroscopic methods.[16] Ligand dissociation from a tetrahedrally co-ordinated zerovalent nickel **I** generates a trigonal, highly reactive NiL_3 species **II**, which undergoes rapid oxidative addition of HCN. The resulting complex **III** with a hydride and a cyano ligand co-ordinating in *trans* positions can easily lose a second monodentate ligand P to yield the tetrahedral species **IV**. Depending on the steric bulk of the ligands P the hydridocyano intermediate **IV** can also adopt a square planar structure. The cycle is continued by olefin co-ordination **V** and insertion of the substrate into the nickel–hydrogen bond giving another tetrahedral intermediate **VI**. Similar to **IV** it should be possible that the cyanoalkyl species **VI** can have a square planar geometry as well. In the last step, reductive elimination takes place to form the product nitrile and the cycle is completed by generating the active complex **II** again.

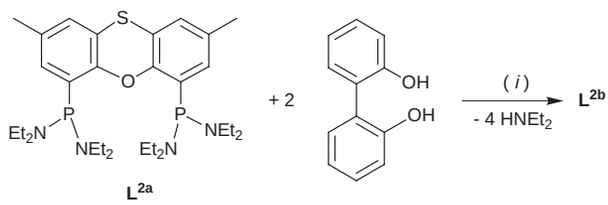

Scheme 3 (*i*) toluene, 90 °C, 15 h

Deactivation of the catalyst is often noticed by the formation of dicyanonickel(II) species **VII**, preferably with the cyano ligands occupying *trans* positions at the metal. All other intermediates of the catalytic cycle favour P–Ni–P angles of either 109° together with tetrahedral geometry or 120° with trigonal structures. When monodentate ligands are used the complexes are very flexible to structural changes, but also highly susceptible to dissociation and catalyst deactivation. Consequently, our conception was focussed on ligands with large natural bite angles and rigid backbones. These Xantphos bidentates should suppress the formation of dicyano complexes **VII**, stabilise the substantially tetrahedral intermediates **IV** and **VI** and thus enhance the reductive elimination and the overall catalysis.[17] Since our aim was the detailed investigation of electronic properties, we selected the phenoxathiine backbone and the Thixantphos ligand L^{1d} respectively for further modification.

Synthesis and molecular modeling

Next to a whole series of Thixantphos diphosphines L^{1a}–L^{1g} that were modified only at the *para* positions of the diphenylphosphanyl moiety, a new diphosphonite ligand L^{2b} was synthesized (Scheme 1). This latter ligand is much less basic at the phosphorus atoms because of the biphenyl oxygen substituents.

The diphosphonite ligand L^{2b} is readily accessible by the reaction of the amido phosphonito phenoxathiine L^{2a} with 2 equivalents of 2,2′-dihydroxy-1,1′-biphenyl (Scheme 3).

The geometries of the ligands were simulated by molecular modeling based on force field calculations.[13] Since the diphosphines L^{1a}–L^{1g} are only modified at the *para* positions of the phenyl substituents, the calculated natural bite angles for nickel complexes are within a very narrow range of 112.8 to 114.5°, except for L^{1a}. A steric influence on the hydrocyanation results can be excluded. Only ligand L^{1a} with dimethylamino groups requires a somewhat larger angle of 118.6°. For the diphosphonite ligand L^{2b} we calculated a bite angle of 120.4°. We suppose that this value is enforced by the limited flexible ring structures of the biphenoxy groups and their steric demand.

Crystal structures

The molecular structure of ligand L^{1d} is drawn in Fig. 1, together with the atom numbering scheme, while selected bond lengths and angles are given in Table 1. The structure clearly shows that only very little adjustment of the ligand is necessary

Table 1 Selected bond lengths (Å) and angles (°) for ligand L^{1d} with estimated standard deviations in parentheses

S–C(6)	1.763(3)	S–C(7)	1.760(3)
P(1)–C(2)	1.846(3)	P(1)–C(20)	1.841(3)
P(1)–C(30)	1.823(3)	P(2)–C(11)	1.836(3)
P(2)–C(40)	1.824(3)	P(2)–C(50)	1.824(3)
O–C(1)	1.371(3)	O–C(12)	1.375(3)
C(4)–C(13)	1.510(4)	C(9)–C(14)	1.518(5)
C(6)–S–C(7)	101.4(1)	P(2)–C(40)–C(45)	117.3(3)
C(2)–P(1)–C(20)	100.5(1)	C(20)–P(1)–C(30)	103.2(1)
C(11)–P(2)–C(40)	101.6(1)	P(2)–C(11)–C(10)	125.1(2)
C(1)–O–C(12)	124.3(2)	O–C(1)–C(2)	115.9(2)
O–C(1)–C(6)	123.4(2)	O–C(12)–C(7)	124.4(2)
O–C(12)–C(11)	114.4(2)	S–C(6)–C(1)	123.4(2)
S–C(6)–C(5)	117.3(2)	P(2)–C(50)–C(51)	115.6(2)
P(2)–C(50)–C(55)	126.5(2)	P(2)–C(40)–C(41)	124.9(2)

Table 2 Selected bond lengths (Å) and angles (°) for complex **1** with estimated standard deviations in parentheses

Ni–Cl(1)	2.191(2)	Ni–Cl(2)	2.206(2)
Ni–P(1)	2.307(2)	Ni–P(2)	2.304(2)
S–C(6)	1.767(6)	S–C(7)	1.758(6)
P(1)–C(2)	1.829(6)	P(1)–C(20)	1.826(6)
P(1)–C(30)	1.823(6)	O–C(1)	1.386(6)
O–C(12)	1.397(6)	C(4)–C(13)	1.497(8)
P(1)···P(2)	3.77	Ni···O	3.37
Cl(1)–Ni–Cl(2)	132.37(7)	Cl(1)–Ni–P(1)	105.82(7)
Cl(1)–Ni–P(2)	102.88(7)	Cl(2)–Ni–P(1)	103.03(7)
Cl(2)–Ni–P(2)	102.08(7)	P(1)–Ni–P(2)	109.52(6)
C(6)–S–C(7)	98.2(3)	Ni–P(1)–C(2)	116.8(2)
Ni–P(1)–C(20)	108.3(2)	Ni–P(1)–C(30)	116.8(2)
C(2)–P(1)–C(20)	103.0(3)	C(2)–P(1)–C(30)	105.7(3)
C(20)–P(1)–C(30)	104.7(3)	C(1)–O–C(12)	116.2(5)

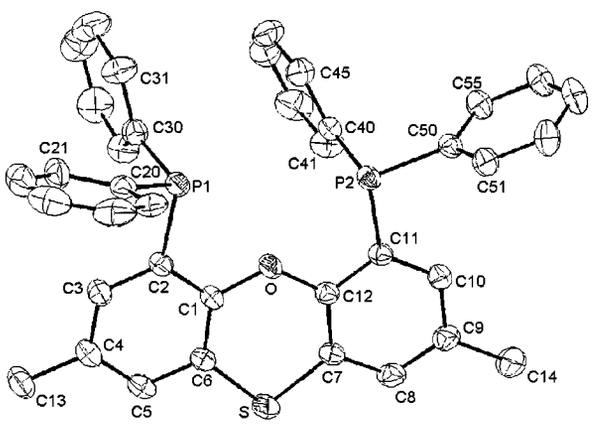

Fig. 1 Molecular structure of ligand **1d**

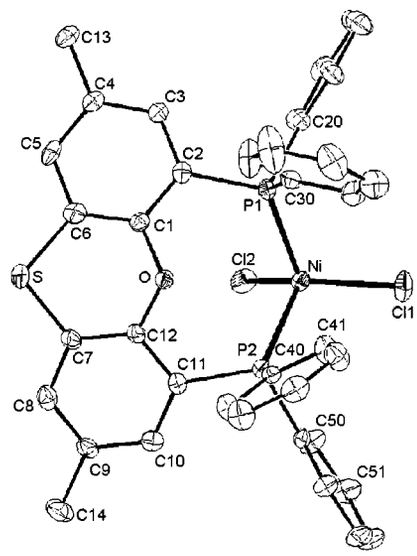

Fig. 2 Molecular structure of complex **1**

to form a chelate complex since the orientation of the diphenylphosphanyl moieties is nearly ideal for metal co-ordination. The non-bonding P···P distance is 4.02 Å. While molecular modeling calculations suggest a bending in the phenoxathiine moiety, the two aromatic rings in the backbone of Thixantphos L^{1d} are coplanar to each other. Probably, the planarity in the solid state arises from crystal structure packing effects. Simulated structures are just idealised gas phase molecules with no interaction to other compounds.

In contrast, the dihedral angle between the two phenyl planes in the backbone of the related Xantphos ligand (CMe_2 instead of S, H instead of Me) is 158°, determined by X-ray analysis.[10,18] π-Stacking interactions between the phenyl substituents at the phosphorus atoms are thought to be responsible for this bending.[19,20]

Despite the numerous bidentate phosphorus ligands known in the literature, only a few dichloro nickel complexes have been characterised by X-ray analysis. Most common geometries to be found for [$NiCl_2$(P–P)] are tetrahedral[21] and square planar.[22] The molecular structure and numbering scheme for complex [$NiCl_2L^{1d}$] **1** are given in Fig. 2. Selected bond lengths, non-bonding distances and angles are presented in Table 2. The compound is paramagnetic which made recording of NMR spectra impossible. Complex **1** was simulated by molecular mechanics and predicted to have a distorted tetrahedral geometry around the metal. The calculated P–Ni–P angle is 110.6° which is in very good agreement with the X-ray determined angle of 109.52(6)°. The backbone bending also could be predicted with a C–S–C angle of 97.4° and a C–O–C angle of 114.6° [X-ray: 98.2(3) and 116.2(5)° respectively]. The dihedral angle between the two aromatic rings in the phenoxathiine moiety is 147.7(3)°.

The bond distances Ni–P [2.307(2) and 2.304(2) Å] appear quite normal compared with the values of 2.28 Å found for [$NiCl_2(PPh_3)_2$][23] and 2.333 Å (average) for [$NiBr_2(PPh_3)_2$].[24] Although the bite angle P–Ni–P of 109.52(6)° is ideal for a tetrahedral geometry around the nickel, the structure is significantly distorted with a Cl–Ni–Cl angle of 132.37(7)° due to the lone-pair repulsion between the two chlorine atoms. A similar geometry was found in the complexes [$NiCl_2$(pop)][25] [pop = 2,2′-bis(diphenylphosphino)diethyl ether] and [$NiCl_2$(diop)][26] [diop = 4,5-bis(diphenylphosphinomethyl)-2,2-dimethyl-1,3-dioxolane] with Cl–Ni–Cl angles of 127.1(2) and 130° respectively. A discussion of distortion of nickel(II) tetrahedra in terms of ligand field theory has been given by Venanzi.[27]

The complex [$Ni(CN)_2L^{1a}$] **2** represents the first known crystal structure of a monomeric dicyanonickel(II) complex with a P–P chelating ligand (Fig. 3 and Table 3). Even complexes of the type [$Ni(CN)_2L_2$] (L = monodentate phosphorus ligand) have been determined by X-ray analysis very rarely.[28] Related dimeric species with bidentate ligands were described by Holah *et al.*,[29] [$Ni_2(CN)_2$(dppm)$_2$], and by Manojlovic-Muir *et al.*,[30] [$Ni_2(CN)_4(Me_2PCH_2PMe_2)_2$], only the latter being characterised by X-ray diffraction. While the calculated natural bite angle for the ligand L^{1a} is 118.6°, the P–Ni–P angle found in the complex **2** is widened to 151.51(5)°. This value is out of the flexibility range[31] for Xantphos type ligands, which is typically about 35° for an excess strain energy of 15 kJ mol^{-1}.[10] The two cyano groups occupy *trans* positions at the nickel with a C–Ni–C angle of 161.0(2)°. Considering the small Ni–O distance of 2.72 Å and the four angles P–Ni–C in the range of 89.8(1) to 95.9(1)°, the geometry around the metal can be described as distorted square pyramidal with the oxygen on

Table 3 Selected bond lengths (Å) and angles (°) for complex **2** with estimated standard deviations in parentheses

Ni–P(1)	2.208(1)	Ni–P(2)	2.197(1)
Ni–C(1)	1.863(5)	Ni–C(2)	1.861(5)
S–C(15)	1.764(5)	S–C(16)	1.760(5)
P(1)–C(11)	1.840(4)	P(1)–C(30)	1.813(4)
P(1)–C(40)	1.808(5)	P(2)–C(20)	1.829(4)
P(2)–C(50)	1.806(4)	P(2)–C(60)	1.795(4)
O–C(10)	1.410(5)	O–C(21)	1.385(5)
N(1)–C(1)	1.154(6)	N(2)–C(2)	1.145(6)
N(3)–C(33)	1.379(6)	N(3)–C(36)	1.475(7)
N(5)–C(53)	1.363(6)	N(5)–C(56)	1.442(6)
P(1) · · · P(2)	4.27	Ni–O	2.72
P(1)–Ni–P(2)	151.51(5)	C(1)–Ni–C(2)	161.0(2)
P(1)–Ni–C(1)	90.5(1)	P(1)–Ni–C(2)	95.9(1)
P(2)–Ni–C(1)	89.8(1)	P(2)–Ni–C(2)	93.0(1)
C(15)–S–C(16)	98.5(2)	C(10)–O–C(21)	117.3(3)
Ni–C(1)–N(1)	173.9(4)	Ni–C(2)–N(2)	172.1(4)
Ni–P(1)–C(11)	105.2(1)	Ni–P(1)–C(30)	122.4(2)
Ni–P(1)–C(40)	115.9(1)	Ni–P(2)–C(20)	105.9(2)
Ni–P(2)–C(50)	117.1(1)	Ni–P(2)–C(60)	118.9(2)

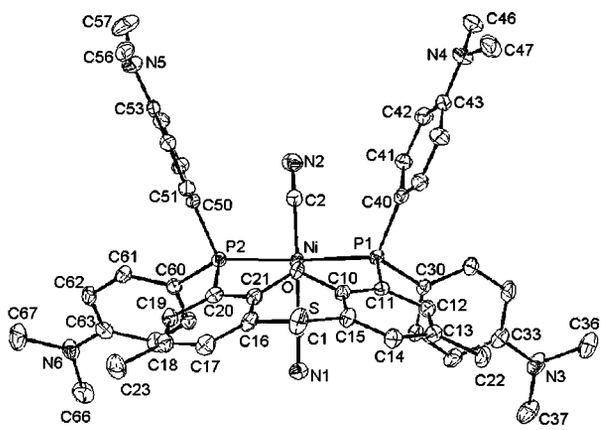

Fig. 3 Molecular structure of complex **2**

top. However, an interaction between the nickel and the oxygen cannot be predicted from the crystal structure only. For nickel complexes with ether ligands found in the Cambridge Crystallographic Database the average Ni–O distance is 2.15 Å. The metal–phosphorus and –carbon bond lengths are in good agreement with those observed in other dicyano d^8-nickel complexes.[32] Both of the Ni–C–N linkages are slightly distorted from ideal linearity with angles of 173.9(4) and 172.1(4)°. The backbone of the ligand is bent by the dihedral angle of 33.6(3)°.

Ligand L^{1a} is the most basic out of the series of diphosphines and the only one that formed a dicyano complex with nickel. We assign that to the electron-donating capability towards the $Ni(CN)_2$ system.

Catalytic hydrocyanation of styrene

Reactions of the Thixantphos ligands L^{1a}–L^{1g} and L^{2b} with 1 equivalent $[Ni(cod)_2]$ yield active catalyst precursors for the hydrocyanation of styrene (Table 4). The compounds L^{1a}–L^{1c} are more basic at the phosphorus atoms than the unsubstituted ligand L^{1d}, caused by a positive mesomeric effect of the amino and methoxy groups and a positive inductive effect of the methyl group. Less basic than Thixantphos L^{1d} are the halogen derivatives L^{1e}–L^{1g} (with R = F, Cl or CF_3). Nevertheless, the negative inductive effect of Cl is reduced by a positive mesomeric effect.

The electron-rich diphosphines L^{1a}–L^{1c} (entries 1–3, Table 4) lead to lower activities in catalytic experiments than the unsubstituted Thixantphos L^{1d}. Best results are obtained with the most electron-poor diphosphine L^{1g} (entry 7, R = CF_3). The

Table 4 Catalytic hydrocyanation of styrene[a]

Entry	Ligand	Conversion[b] (%)	Yield[b] (%)	Selectivity[b] (%)	Regioselectivity[b] (%)
1	L^{1a}	16	12	76	>99
2	L^{1b}	33	22	66	99.5
3	L^{1c}	55	48	87	99.8
4	L^{1d}	77	70	92	99.4
5	L^{1e}	46	38	83	99.4
6	L^{1f}	75	52	70	99.3
7	L^{1g}	98	90	92	99.0
8	L^{2b}	49	47	97	99.4

[a] Reaction conditions: toluene (2 cm^3), nickel : ligand : styrene : HCN = 1 : 1.05 : 20 : 25; 60 °C, 16 h, preformation time = 30 min. [b] Conversion (based on the substrate); yield, selectivity and regioselectivity determined by temperature-controlled GC analysis. Regioselectivity is defined as the percentage of branched nitrile.

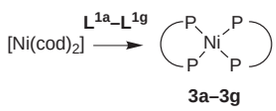

3a–3g

Scheme 4 Formation of bis-chelate nickel complexes

other two halogen derivatives L^{1e} and L^{1f} perform less successfully than expected (entries 5 and 6). A plausible explanation may be that ligand decomposition has occurred by reaction of the aryl halogenides with styrene mediated by nickel species. Similar Heck type reactivity is best known with palladium.[33] We have observed the same deactivation mechanism with nickel complexes in the presence of chlorinated or brominated aromatic substrates. The fluoride in ligand L^{1g} is not bound directly to an aromatic ring and therefore inert towards reaction with the metal of the catalyst. Moderate yield combined with a very high selectivity is obtained in the presence of the diphosphonite ligand L^{2b} (entry 8). This unprecedented behaviour will be explained later.

With styrene as a substrate, the branched nitrile is the strongly favoured product over the linear one. This regioselectivity is attributed to stabilisation of the branched alkyl intermediate by a η^3-benzyl interaction of the nickel.[2] Still, the selectivity induced by the Thixantphos ligands L^{1a}–L^{1g} and L^{2b} (>99%) is significantly higher than those obtained with common diphosphines (up to 95%)[8] and the commercial *o*-tolyl phosphite system (91%),[34] and comparable to that of diphosphonites based on sugar backbones.[35]

NMR characterisation of nickel complexes

Various *in situ* catalyst solutions were investigated by means of ^{31}P-{^1H} NMR spectroscopy. Surprisingly, the addition of either 1 or 2 equivalents of Thixantphos diphosphine ligands L^{1a}–L^{1g} to toluene solutions of $[Ni(cod)_2]$ resulted in similar spectra. The complexity of the peak pattern observed can only be explained by multiple couplings between various phosphorus atoms. The species which are responsible for this are the bis(chelate) complexes [Ni(P–P)$_2$] **3a**–**3g** (Scheme 4). The ^{31}P-{^1H} NMR spectrum of complex **3d** (P–P = Thixantphos L^{1d}) was simulated with g-NMR software[36] (Fig. 4). The peak pattern could most accurately be simulated by an AA′XX′ system with four large coupling constants of 50 Hz and two smaller ones of 12.5 Hz (Table 5). Therefore the structure of complex **3d** is supposed to be distorted tetrahedral.

The complex peak pattern at 273 K is caused by a highly asymmetric geometry of the bis(chelate) complex **3d**. We conclude that due to the non-planarity of the ligand backbones there are at least two different co-ordination modes (Scheme 5), which make the phosphorus nuclei P_a and P_b magnetically inequivalent. With a fixed roof-like co-ordination of the first

Table 5 Chemical shifts and *J*(PP) values of the NMR simulation for [NiL$^{1d}_2$] **3d**

		J/Hz		
Nucleus	δ	1	2	3
P^1	15.00			
P^2	11.70	50		
P^3	15.00	50	12.5	
P^4	11.70	12.5	50	50

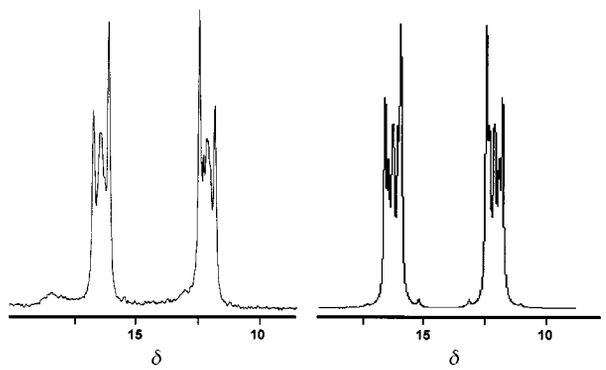

Fig. 4 Recorded (left, 273 K, toluene-d_8) and simulated (right) ^{31}P-{^{1}H} NMR spectra of [NiL$^{1d}_2$] **3d**

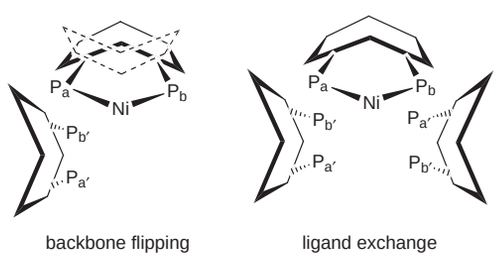

Scheme 5 Possible coordination modes and exchange processes of a bis-chelate complex (phenyl groups are omitted for clarity)

equivalent of ligand the backbone of the second diphosphine can be folded either to the left or to the right side. These two species are enantiomeric complexes. However, since there are two diastereotopic phosphorus atoms, the ^{31}P-{^{1}H} NMR spectrum shows two different chemical shifts for P_a and P_b at δ 11.7 and 15.0 respectively.

Subsequently, the bis(chelate) complex [NiL^{1d}] **3d** was investigated in detail by variable temperature ^{31}P-{^{1}H} NMR as shown in Fig. 5. On heating the sample from room temperature to 371 K, line broadening occurs caused by a fluxional process and the phosphorus atoms become magnetically equivalent, with a coalescence temperature of 353 K. For this exchange process a butterfly flipping of the ligand backbones as well as ligand dissociation can be proposed. At higher temperatures this process is fast in comparison to the $\nu(P_a) - \nu(P_b)$ frequency separation. Especially since the bis(chelate) complex is as catalytically active as the monochelate complex [Ni(cod)L^{1d}], ligand dissociation cannot be excluded as a reason for the fluxionality.

From the recorded and simulated ^{31}P-{^{1}H} NMR spectra, the rate constants (k) for the fluxional process have been determined for complex **3d**. In the Eyring plot in Fig. 6 the rate constants (k) for phosphorus exchange are given as a function of the NMR sample temperature for **3d**. From the Eyring equation and the Eyring plot, the thermodynamic values for the activation of the dynamic process were calculated. The assumption used is that $\Delta H^‡$ and $\Delta S^‡$ are constant over the temperature range (293–371 K) employed. The enthalpy of activation $\Delta H^‡$ is 61.4 kJ mol^{-1} and the entropy of activation

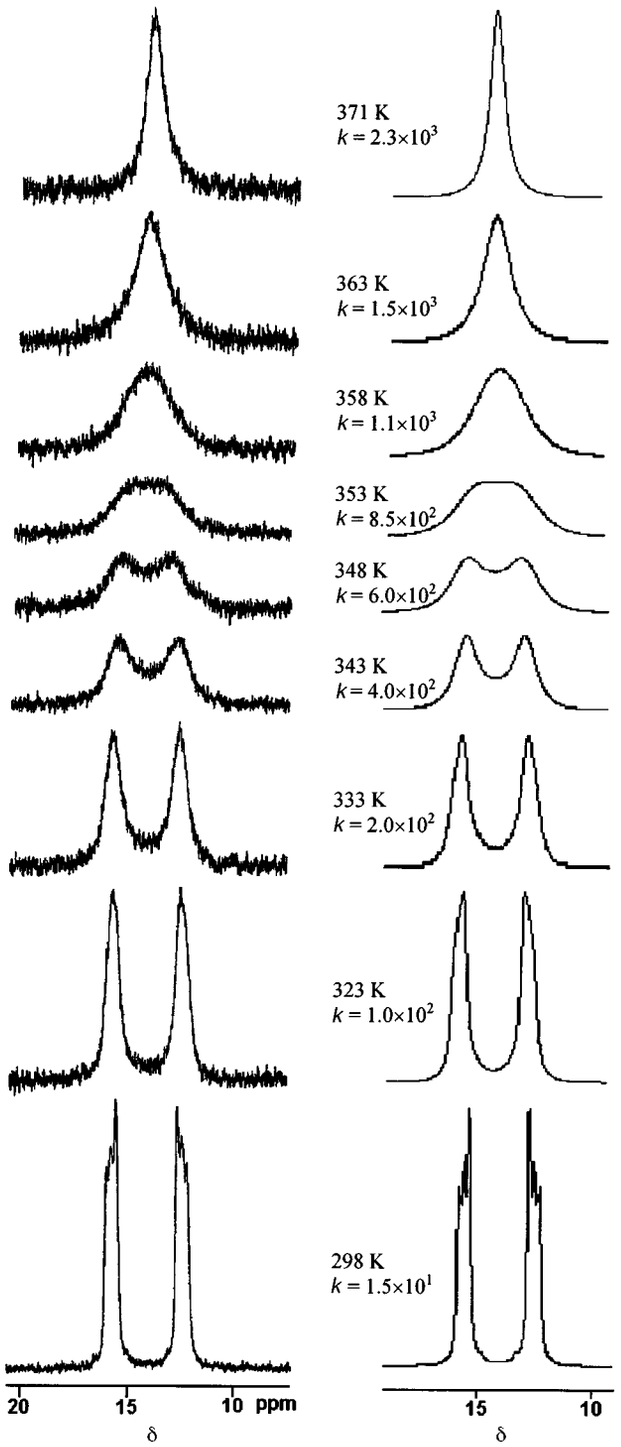

Fig. 5 Variable temperature ^{31}P-{^{1}H} NMR spectrum (toluene-d_8) of [NiL$^{1d}_2$] **3d**, recorded (left) and simulated (right)

$\Delta S^‡$ is -16.7 K^{-1} mol^{-1}. The latter value is relatively small, indicative of an intramolecular rearrangement process, thus a butterfly flipping of the ligand backbones. For a temperature of 293 K, the free energy value $\Delta G^‡ = 66.3$ kJ mol^{-1} has been determined from the Gibbs equation $\Delta G^‡ = \Delta H^‡ - T\Delta S^‡$.

When our investigations were extended to the Thixantphos diphosphonite L^{2b} a similar behaviour was observed. The ^{31}P-{^{1}H} NMR spectrum ([$^2H_8$]toluene, 298 K) of an *in situ* catalyst solution containing equimolar amounts of [Ni(cod)$_2$] and ligand L^{2b} shows a singlet at δ 196.6 5 min after mixing, resulting from the monochelate [Ni(cod)L^{2b}]. After 30 min, about 80% of the ligand has already formed the bis(chelate) complex [NiL$^{2b}_2$] **4** showing two pseudo-triplet signals at δ 187.5 and 177.6 (Fig. 7). Surprisingly, NMR simulation for complex **4** requires equal

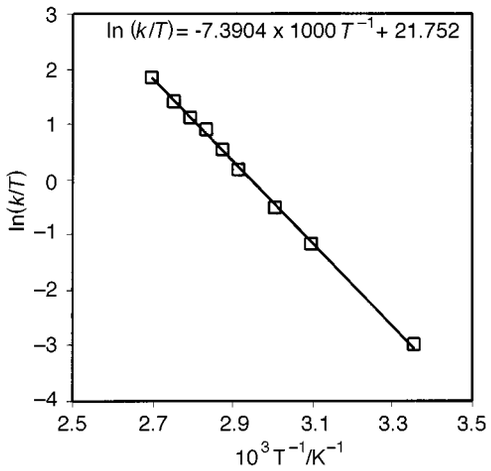

Fig. 6 Eyring plot: data obtained from variable-temperature ^{31}P-{^{1}H} NMR of [NiL$^{1d}_2$] **3d**

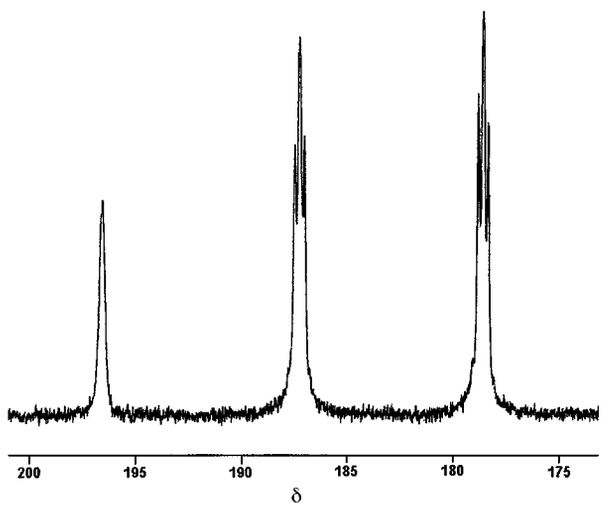

Fig. 7 ^{31}P-{^{1}H} NMR spectrum (toluene-d_8, 298 K) of *in situ* catalyst preformation with [Ni(cod)$_2$] and 1 equivalent of ligand L^{2b}, recorded 30 minutes after mixing

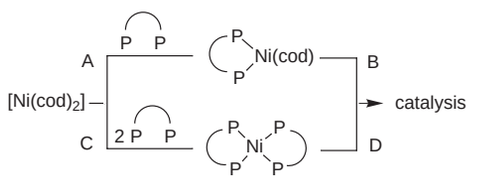

Scheme 6 Pathways of *in situ* catalyst preformation

$^{2}J(P_aP_{a'})$, $^{2}J(P_aP_b)$, $^{2}J(P_aP_{b'})$, $^{2}J(P_bP_{b'})$ couplings of 27 Hz suggesting a structure of high symmetry. The bis(chelate) complex **4** is very stable. Heating to 373 K does not change the signals in the ^{31}P-{^{1}H} NMR spectrum. Furthermore, **4** is catalytically inactive up to 423 K.

Together with the results obtained in the hydrocyanation of styrene, the NMR spectra of the catalyst solutions allow a deeper insight into the pathways of catalyst activity and deactivation for the various ligands (Scheme 6). The chelating Thixantphos ligands L^{1a}–L^{1g} and L^{2b} preferably form bis(chelates) *via* route **C**, even if they are added substoichiometrically. In the case of the diphosphines L^{1a}–L^{1g} the bis(chelate) nickel complexes **3a**–**3g** are still catalytically active since dissociation of the ligand occurs even at room temperature (route **D**). In contrast, the bis(chelate) complex [NiL$^{2b}_2$] **4** is uncommonly stable and therefore not active in catalysis. High conversion of the substrate is only possible when the preformation time is short and the active catalyst precursor [Ni(cod)L^{2b}] is still present in large amounts (routes **A** and **B**). Regarding a preformation time of 30 min and a deactivation of about 80% of the nickel, the moderate values for conversion and yield in the presence of ligand L^{2b} given in Table 4 must be reconsidered. Taking all this into account, L^{2b} shows high catalytic activity due to electronic properties.

Conclusion

A series of electronically tuned Thixantphos ligands was applied to the nickel catalysed hydrocyanation of styrene. Electron-withdrawing substituents at the phosphorus atoms make the ligands more acidic and lead to best activities. The concept of large bite angles combined with rigid backbones is demonstrated by their importance for intermediates of the catalytic cycle and is supported by both crystal structures and ^{31}P-{^{1}H} NMR spectroscopy. A diphosphonite Thixantphos ligand with comparable geometry forms highly active nickel complexes. Bis(chelate) complexes of this ligand are very stable and catalytically inactive.

Experimental

Computational details

Molecular mechanics calculations were performed on a Silicon Graphics Indigo2 workstation using SYBYL software and a modified TRIPOS force field.[13] Natural bite angles were calculated using a method similar to that described by Casey and Whiteker,[14] based on a Ni–P bond length of 2.177 Å and a P–Ni–P bending force constant of 0 kcal mol^{-1} degree^{-2} (cal = 4.184 J).

Syntheses

All preparations were carried out under an atmosphere of purified argon using standard Schlenk techniques. Solvents were dried and freshly distilled prior to use. 2,8-Dimethylphenoxathiine and the diphosphines L^{1a}–L^{1g} were prepared as described in recent publications.[10] The compound [Ni(cod)$_2$] was synthesized according to literature methods.[37] The NMR spectra were recorded on a Bruker DPX300 spectrometer (^{1}H, 300; ^{13}C, 75; ^{31}P, 121 MHz).

Hydrogen cyanide. CAUTION: HCN is a highly toxic, volatile liquid (b.p. 27 °C) that is susceptible to exothermic and uncontrolled polymerisation in the presence of basic catalysts. It should be handled only in a well ventilated fume hood and by teams of at least two technically qualified persons who have received appropriate medical training for treating HCN poisoning. Sensible precautions include also the use of HCN monitoring equipment. It can be generated by the addition of H_2SO_4 to sodium cyanide. Uninhibited HCN should be stored at a temperature lower than its melting point (−13 °C).

4,6-Bis(diethylaminophosphino)-2,8-dimethylphenoxathiine L^{2a}. 2,8-Dimethylphenoxathiine (3.26 g, 14.3 mmol) and *N*,*N*,*N*′,*N*′-tetramethylethane-1,2-diamine (4.14 g) were dissolved in diethyl ether (50 cm^3) and cooled to 230 K. *n*-Butyllithium (14.3 cm^3 of a 2.5 M solution in hexanes, 35.7 mmol) was added slowly, giving a bright yellow solution. The mixture was stirred at room temperature for 16 h and then added to a solution of chlorobis(diethylamino)phosphine (6.32 g, 35.7 mmol) in pentane (30 cm^3) at 230 K. After stirring for 16 h at room temperature and evaporating the solvents a crude yellow product was obtained. The compound L^{2a} was recrystallised from pentane, yield 3.90 g (48%) (Found: C, 61.6; H, 8.60; N, 9.3. $C_{30}H_{50}N_4OP_2S$ requires C, 62.5; H, 8.75; N, 9.7%). NMR (C_6D_6): ^{1}H, δ 7.28 (s, 2 H), 6.74 (s, 2 H), 3.21 (m, 16 H, CH_2), 2.09 (s, 6 H, CH_3) and 1.13 (t, 12 H, ^{3}J 7.0 Hz); ^{13}C-{^{1}H},

δ 151.0, 132.8, 131.0, 127.7, 127.1, 118.9, 43.5 (CH_2), 20.7 (CH_3) and 14.8 (CH_2CH_3); ^{31}P-{^{1}H}, δ 90.4.

4,6-Bis(dibenzo[*d*,*f*][1,3,2]dioxaphosphepino-1-yl)-2,8-dimethylphenoxathiine L^{2b}. Compound L^{2a} (577 mg, 1.0 mmol) and dihydroxybiphenyl (372 mg, 2.0 mmol) were dissolved in toluene (5 cm^3) and the solution was stirred at 383 K for 15 h. The mixture was allowed to evaporate to dryness to give a bright yellow crystalline product, yield 650 mg (99%), m.p. >260 °C (Found: C, 69.1; H, 4.25. $C_{38}H_{26}O_5P_2S$ requires C, 69.5; H. 4.00%). NMR ($CDCl_3$): ^{1}H, δ 7.33 (d, ^4J 2.1, 2 H), 7.30 (d, ^4J 2.4, 2 H), 7.18–7.09 (m, 8 H), 6.96 (d, ^4J 1.8 Hz, 2 H), 6.93–6.90 (m, 6 H) and 2.01 (s, 6 H, CH_3); ^{13}C-{^{1}H}, δ 152.2, 151.4, 134.0, 132.0, 130.0, 129.8, 129.4, 129.0, 128.8, 122.1, 119.4 and 20.5 (CH_3); ^{31}P-{^{1}H}, δ 178.3.

[NiCl$_2$L^{1d}] 1. Ligand L^{1d} (853 mg, 1.43 mmol) and nickel(II) dichloride hexahydrate (340 mg, 1.43 mmol) were suspended in benzene (10 cm^3) and stirred at 323 K for 3 h. Evaporating the solvent gave a reddish brown solid in quantitative yield. Red crystals suitable for X-ray analysis were obtained from boiling benzene, m.p. >260 °C (Found: C, 64.0; H, 4.37. $C_{38}H_{30}Cl_2NiOP_2S$ requires C, 62.8; H, 4.16%).

[Ni(CN)$_2$L^{1a}] 2. One large blue crystal of complex **2** was isolated from a toluene solution (2 cm^3) of a catalytic experiment after standing for several days at room temperature. Before catalysis, the solution contained [Ni(cod)$_2$] (17.9 mg, 0.065 mmol), ligand L^{1a} (53.6 mg, 0.070 mmol), styrene (135.4 mg, 1.3 mmol) and hydrogen cyanide (42 mg, 1.625 mmol).

Catalytic hydrocyanation of styrene

In a typical experiment, a bright yellow 0.065 mM solution of [Ni(cod)$_2$] in toluene (2 cm^3) was added to a Schlenk tube containing a stirring bar and 1.05 equivalents of ligand. The mixture was stirred for 30 min to ensure complete formation of the catalyst precursor. Then styrene (1.3 mmol) was added. The solution was cooled to 220 K, liquid HCN (63 µl, 1.625 mmol) was added at once and the tube was placed in a heating bath. After 16 h at 333 K the excess of HCN was removed by a gentle stream of argon, solid particles were removed by centrifugation and the remaining solution was analysed by temperature-controlled gas chromatography.

Crystallography

Colourless crystals of ligand L^{1d} were obtained from boiling acetone, red crystals of complex **1** from boiling benzene. Blue crystals of complex **2** were isolated from a catalysis experiment applying ligand L^{1a} as described earlier.

Data were collected on a CAD-4 diffractometer (graphite monochromator) and ω–2θ scans. Structure solution was by direct methods. Full-matrix least-squares refinement on F was carried out with anisotropic displacement parameters for all non-hydrogen atoms. Hydrogen atoms were placed in idealised positions with isotropic displacement parameters of U(H) = 1.3B(C) and allowed to ride on their C atoms. Calculations were performed using the SDP system of programs.[38]

L^{1d}. $C_{38}H_{30}OP_2S$, M_r 596.67, monoclinic, space group $P2_1/c$, a = 11.904(2), b = 21.377(2), c = 13.285(2) Å, β = 112.18(1)°, U = 3130.4(7) Å^3, D_c = 1.266 g cm^{-3}, Z = 4, F(000) 1248, λ(Cu–Kα) = 1.541 84 Å. Crystal size 0.40 × 0.25 × 0.20 mm.

A total of 9557 reflections were collected at 293 K in the range 5.0 < θ < 75.0°, corresponding to 4989 unique data with $I > 1.0\sigma(I)$, which were used for further computations. An empirical absorption correction based on ψ scans was applied. Refinement converged with 499 parameters using a statistical weighting scheme at values of R = 0.062 and R' = 0.063 with a goodness of fit of 1.280.

Complex 1. $C_{38}H_{30}Cl_2NiOP_2S{\cdot}3C_6H_6$, M_r 960.63 (including solvent of crystallisation), monoclinic, space group $P2_1/c$, a = 19.755(8), b = 19.314(8), c = 13.072(3) Å, β = 103.14(3)°, U = 4857(3) Å^3, D_c = 1.314 g cm^{-3}, Z = 4, F(000) 2000, λ(Mo-Kα) = 0.710 73 Å. Crystal size 0.40 × 0.15 × 0.20 mm.

A total of 12 207 reflections were collected at 203 K in the range 2.0 < θ < 25.0°, corresponding to 5601 unique data with $I > 1.0\sigma(I)$, which were used for further computations. An empirical absorption correction based on ψ scans was applied. Refinement converged with 568 parameters using a statistical weighting scheme at values of R = 0.085 and R' = 0.065 with a goodness of fit of 1.173.

Complex 2. $C_{48}H_{50}N_6NiOP_2S{\cdot}2C_7H_8$, M_r 1063.98 (including solvent of crystallisation), triclinic, space group $P\bar{1}$, a = 11.436(5), b = 12.496(3), c = 21.699(8) Å, α = 77.20(2), β = 86.18(3), γ = 65.86(2)°, U = 2758(2) Å^3, D_c = 1.282 g cm^{-3}, Z = 2, F(000) 1124, λ(Mo-Kα) = 0.710 73 Å. Crystal size 0.52 × 0.48 × 0.28 mm.

A total of 10 824 reflections were collected at 203 K in the range 2.0 < θ < 25.0°, corresponding to 7164 unique data with $I > 1.0\sigma(I)$, which were used for further computations. Refinement converged with 658 parameters using a statistical weighting scheme at values of R = 0.081 and R' = 0.072 with a goodness of fit of 1.414.

CCDC reference number 186/1065.

See http://www.rsc.org/suppdata/dt/1998/2981/ for crystallographic files in .cif format.

Acknowledgements

Financial support from the E.U. Human Capital and Mobility Program (MMCOS Network) and the Dutch Foundation for Chemical Research and Foundation for Technological Sciences (SON/STW) is gratefully acknowledged.

References

1 K. Huthmacher and S. Krill, in *Applied Homogeneous Catalysis with Organometallic Compounds*, eds. B. Cornils and W. A. Hermann, VCH, Weinheim, 1996, p. 465.
2 R. J. McKinney, in *Homogeneous Catalysis*, ed. G. W. Parshall, Wiley, New York, 1992, p. 42.
3 W. C. Drinkard (DuPont), *US Pat.*, 3 766 237, 1973; M. Rapoport (DuPont), *US Pat.*, 4 371 474, 1983; W. Tam (DuPont), *US Pat.*, 5 543 536, 1996.
4 K. A. Kreutzer and W. Tam (DuPont), *US Pat.*, 5 512 696, 1996; A. I. Breikss (DuPont), *US Pat.*, 5 523 453, 1996; K. A. Kreutzer and W. Tam (DuPont), *US Pat.*, 5 663 369, 1997; W. Tam, K. A. Kreutzer and R. J. McKinney (DuPont), *US Pat.*, 5 688 986, 1997.
5 M. J. Baker, K. N. Harrison, A. G. Orpen, P. G. Pringle and G. Shaw, *J. Chem. Soc.*, *Chem. Commun.*, 1991, 803; M. J. Baker and P. G. Pringle, *J. Chem. Soc.*, *Chem. Commun.*, 1991, 1292.
6 A. L. Casalnuovo, T. V. RajanBabu, T. A. Ayers and T. H. Warren, *J. Am. Chem. Soc.*, 1994, **116**, 9869.
7 T. V. RajanBabu and A. L. Casalnuovo, *J. Am. Chem. Soc.*, 1996, **118**, 6325.
8 M. Kranenburg, P. C. J. Kamer, P. W. N. M. van Leeuwen, D. Vogt, and W. Keim, *J. Chem. Soc.*, *Chem. Commun.*, 1995, 2177.
9 W. Goertz, P. C. J. Kamer, P. W. N. M. van Leeuwen and D. Vogt. *Chem. Commun.*, 1997, 1521.
10 M. Kranenburg, Y. E. M. van der Burgt, P. C. J. Kamer, P. W. N. M. van Leeuwen, K. Goubitz and J. Fraanje, *Organometallics*, 1995, **14**, 3081; M. Kranenburg, P. C. J. Kamer, P. W. N. M. van Leeuwen and B. Chaudret, *Chem Commun.*, 1997, 373; M. Kranenburg, J. G. P. Delis, P. C. J. Kamer, P. W. N. M. van Leeuwen, K. Vrieze, A. L. Spek, K. Goubitz and J. Fraanje, *J. Chem. Soc.*, *Dalton Trans.*, 1997, 1839.
11 M. Kranenburg, P. C. J. Kamer and P. W. N. M. van Leeuwen, *Eur. J. Inorg. Chem.*, 1998, **1**, 25; **2**, 155.
12 C. A. Tolman, *J. Chem. Educ.*, 1986, **63**, 199.
13 SYBYL, version 6.3, TRIPOS Associates, St. Louis, MO, 1996.
14 C. P. Casey and G. T. Whiteker, *Isr. J. Chem.*, 1990, **30**, 299.
15 C. A. Tolman, R. J. McKinney, W. C. Seidel, J. D. Druliner and W. R. Stevens, *Adv. Catal.*, 1985, **33**, 1.

16 C. A. Tolman, *J. Am. Chem. Soc.*, 1970, **92**, 2956; *Inorg. Chem.*, 1971, **10**, 1540; *J. Am. Chem. Soc.*, 1972, **94**, 2994; J. D. Druliner, A. D. English, J. P. Jesson, P. Meakin and C. A. Tolman, *J. Am. Chem. Soc.*, 1976, **98**, 2156; W. R. Jackson and C. G. Lovel, *Aust. J. Chem.*, 1982, **35**, 2053; C. A. Tolman, W. C. Seidel and L. W. Gosser, *Organometallics*, 1983, **2**, 1391; J. E. Bäckvall and O. S. Andell, *Organometallics*, 1986, **5**, 2350; R. J. McKinney and D. C. Roe, *J. Am. Chem. Soc.*, 1986, **108**, 5167.
17 J. M. Brown and P. J. Guiry, *Inorg. Chim. Acta*, 1994, **220**, 249.
18 S. Hillebrand, J. Bruckmann, C. Krüger and M. W. Haenel, *Tetrahedron Lett.*, 1995, **36**, 75.
19 M. Kranenburg, Ph.D. Thesis, University of Amsterdam, 1996.
20 C. A. Hunter and J. K. M. Sanders, *J. Am. Chem. Soc.*, 1990, **112**, 5525.
21 M. D. Fryzuk, P. A. McNeil, S. J. Rettig, A. S. Secco and J. Trotter, *Organometallics*, 1982, **1**, 918.
22 S.-T. Liu, G.-J. Liu, C.-H. Yieh, M.-C. Cheng and S.-M. Peng, *J. Organomet. Chem.*, 1990, **387**, 83; R. Busby, M. B. Hursthouse, P. S. Jarrett, C. W. Lehmann, K. M. A. Malik and C. Philips, *J. Chem. Soc.*, *Dalton Trans.*, 1993, 3767; A. L. Spek, B. P. van Eijck, R. J. F. Jans and G. van Koten, *Acta Crystallogr.*, *Sect. C*, 1987, **43**, 1878; F. Bachechi and L. Zambonelli, *Acta Crystallogr.*, *Sect. C*, 1992, **48**, 788.
23 G. Garton, D. E. Henn, N. M. Powell and L. M. Venanzi, *J. Chem. Soc.*, 1963, 3625.
24 J. A. J. Jarvis, R. H. B. Mais and P. G. Owston, *J. Chem. Soc. A*, 1968, 1473.
25 P. T. Greene and L. Sacconi, *J. Chem. Soc. A*, 1970, 866.
26 V. Gramlich and G. Consiglio, *Helv. Chim. Acta*, 1979, **62**, 1016.
27 L. M. Venanzi, *J. Chem. Soc.*, 1958, 719.
28 B. Corain, M. Basato, G. Favero, P. Rosano and G. Valle, *Inorg. Chim. Acta*, 1984, **85**, L27; H. Hope, M. M. Olmstead, P. P. Power and M. Viggiano, *Inorg. Chem.*, 1984, **23**, 326.
29 D. G. Holah, A. N. Hughes and N. I. Khan, *Can. J. Chem.*, 1984, **62**, 1016.
30 L. Manojlovic-Muir, K. W. Muir and M.-A. Rennie, *Acta Crystallogr.*, *Sect. C*, 1995, **51**, 1533.
31 C. P. Casey, G. T. Whiteker, M. G. Melville, L. M. Petrovich, J. A. Gavney and D. R. Powell, *J. Am. Chem. Soc.*, 1992, **114**, 5535.
32 H. M. Powell, D. J. Watkin and J. B. Wilford, *J. Chem. Soc. A*, 1971, 1803; J. K. Stalick and J. A. Ibers, *Inorg. Chem.*, 1969, **8**, 1090.
33 A. de Meijere and F. E. Meyer, *Angew. Chem.*, *Int. Ed. Engl.*, 1994, **33**, 2379.
34 C. A. Tolman, W. C. Seidel, J. D. Druliner and P. J. Domaille, *Organometallics*, 1984, **3**, 33.
35 T. V. RajanBabu and A. L Casalnuovo, *J. Am. Chem. Soc.*, 1992, **114**, 6265.
36 g-NMR, version 3.6, Ivory Soft, Cherwell Scientific, Oxford, 1996.
37 B. Bogdanovic, M. Kröner and G. Wilke, *Liebigs Ann. Chem.*, 1966, **699**, 1; R. A. Schunn, *Inorg. Synth.*, 1974, **15**, 5.
38 SDP program (Structure Determination Package), V5.0, B. A. Frenz & Associates, Inc., College Station, TX, 1989.

Received 23*rd March* 1998; *Paper* 8/02269K